

## Low temperature plasma etching for Si<sub>3</sub>N<sub>4</sub> waveguide applications

D. Celso, R. Vandusen, T. Smy, J. Albert, N. G. Tarr, and P. D. Waldron

Citation: *Journal of Vacuum Science & Technology A* **26**, 253 (2008); doi: 10.1116/1.2836424

View online: <http://dx.doi.org/10.1116/1.2836424>

View Table of Contents: <http://scitation.aip.org/content/avs/journal/jvsta/26/2?ver=pdfcov>

Published by the AVS: Science & Technology of Materials, Interfaces, and Processing

### Articles you may be interested in

[Low-loss rib waveguides containing Si nanocrystals embedded in SiO<sub>2</sub>](#)

*J. Appl. Phys.* **97**, 074312 (2005); 10.1063/1.1876574

[Scattering loss in silicon-on-insulator rib waveguides fabricated by inductively coupled plasma reactive ion etching](#)

*Appl. Phys. Lett.* **85**, 3995 (2004); 10.1063/1.1815063

[Characterization of sidewall roughness of InP/InGaAsP etched using inductively coupled plasma for low loss optical waveguide applications](#)


*J. Vac. Sci. Technol. B* **21**, 2888 (2003); 10.1116/1.1625956




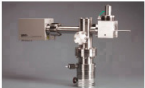
[Technology and realization of metallic curved waveguide mirrors in polymer film waveguides based on anisotropic plasma etching](#)

*J. Vac. Sci. Technol. A* **19**, 87 (2001); 10.1116/1.1335839

[Etch characteristics of optical waveguides using inductively coupled plasmas with multidipole magnets](#)

*J. Vac. Sci. Technol. A* **17**, 1483 (1999); 10.1116/1.581840


Instruments for Advanced Science

<p>Contact Hiden Analytical for further details:  <b>W</b> <a href="http://www.HidenAnalytical.com">www.HidenAnalytical.com</a>  <b>E</b> <a href="mailto:info@hiden.co.uk">info@hiden.co.uk</a></p> <p><b>CLICK TO VIEW</b> our product catalogue</p>	 <p><b>Gas Analysis</b></p> <ul style="list-style-type: none"> <li>› dynamic measurement of reaction gas streams</li> <li>› catalysis and thermal analysis</li> <li>› molecular beam studies</li> <li>› dissolved species probes</li> <li>› fermentation, environmental and ecological studies</li> </ul>	 <p><b>Surface Science</b></p> <ul style="list-style-type: none"> <li>› UHV TPD</li> <li>› SIMS</li> <li>› end point detection in ion beam etch</li> <li>› elemental imaging - surface mapping</li> </ul>	 <p><b>Plasma Diagnostics</b></p> <ul style="list-style-type: none"> <li>› plasma source characterization</li> <li>› etch and deposition process reaction</li> <li>› kinetic studies</li> <li>› analysis of neutral and radical species</li> </ul>	 <p><b>Vacuum Analysis</b></p> <ul style="list-style-type: none"> <li>› partial pressure measurement and control of process gases</li> <li>› reactive sputter process control</li> <li>› vacuum diagnostics</li> <li>› vacuum coating process monitoring</li> </ul>
--	--	--	--	--

# Low temperature plasma etching for Si<sub>3</sub>N<sub>4</sub> waveguide applications

D. Celo,<sup>a)</sup> R. Vandusen, T. Smy, J. Albert, and N. G. Tarr  
*Department of Electronics, Carleton University, Ottawa, Ontario K1S 5B6, Canada*

P. D. Waldron  
*Institute for Microstructural Sciences, NRC 1200 Montreal Road, Ottawa, Ontario K1A 0R6, Canada*

(Received 21 August 2007; accepted 27 December 2007; published 30 January 2008)

Highly selective and anisotropic low temperature electron cyclotron resonance plasma etching process for silicon nitride optical rib waveguide devices compatible with integrated circuit technology is presented. Etching at low temperatures ( $-30\text{ }^{\circ}\text{C}$ ) with SF<sub>6</sub>/O<sub>2</sub> chemistry in combination with a silicon dioxide hard mask achieved good anisotropy with the vertical sidewalls. © 2008 American Vacuum Society. [DOI: 10.1116/1.2836424]

## I. INTRODUCTION

Optical waveguides (WGs) with a silicon nitride (Si<sub>3</sub>N<sub>4</sub>) core surrounded by silicon oxide (SiO<sub>2</sub>) cladding layers represent one of the best alternatives to fabricate planar waveguides with large core-cladding refractive index difference. Low scattering and absorption losses and compatibility with Si processing makes this technology attractive for planar lightwave integrated circuits. While this technology has existed for more than a decade, a reliable fabrication process of silicon nitride waveguides still remains a key issue in obtaining desired optical parameters. The etching process for the formation of the silicon nitride core should be anisotropic, to produce high aspect ratio features with vertical sidewalls, and highly selective to mask material, to minimize the erosion during the etching process. As reported in Ref. 1, carbon-free etching of Si<sub>3</sub>N<sub>4</sub> with SF<sub>6</sub>/O<sub>2</sub>/N<sub>2</sub> gas mixture in high-density electron cyclotron resonance (ECR) plasma source is possible. According to the authors, SiN<sub>x</sub> etch rates of 20–30 nm/min have been achieved with high selectivity over both SiO<sub>2</sub> and Si. However, due to a poor selectivity of the process over the mask material, most of the experiments were limited to 2 min etching time, in order to avoid complete resist removal. Furthermore, no anisotropy was reported, making this process not ideal for Si<sub>3</sub>N<sub>4</sub> waveguide fabrication.

In order to obtain anisotropic etching, the high chemical reactivity of atomic fluorine with silicon or nitride generally demands the use of a sidewall passivant or cryogenic temperatures. As demonstrated for polysilicon applications, SF<sub>6</sub>/O<sub>2</sub> plasmas in which oxyfluorides provide sidewall passivation have achieved some success,<sup>2,3</sup> but are generally viewed to have insufficient anisotropy for waveguide applications. The use of fluorine chemistry at cryogenic substrate temperatures improves the process by further inhibiting lateral etching,<sup>4</sup> leading to high anisotropies with almost vertical sidewalls. A technique for successful etching of silicon with SF<sub>6</sub> plasma at cryogenic substrate temperatures was demonstrated,<sup>5</sup> and has since become widely used for

silicon-on-insulator rib waveguide applications.<sup>6</sup> Several authors<sup>7–9</sup> have studied the effect of different process parameters such as sidewall angle, silicon etch rate, and selectivity to oxide and photoresist (PR) as function of gas flow concentration as well as substrate temperature. In general, the results show that vertical-walled, anisotropic etching of silicon with good selectivity to oxide can be achieved.

As evident from applications to silicon, the aggressive cleaning action of sulfur hexafluoride with added oxygen makes this chemistry a good candidate for use in etching nitride waveguides. Nevertheless, there are problems that should be addressed: SF<sub>6</sub> is not only aggressive to nitride but also to PR. This low selectivity in the process limits etch time and etch depth of the nitride layer and also hinders formation of vertical sidewalls in the nitride ridge waveguide due to the erosion of mask material. The problem is worsened by the presence of oxygen in the plasma, as oxygen plasma etching can strip most solidified PR. Even a small percentage of fluorinated gas can greatly increase the removal rate for many resists.<sup>10</sup> Fluorine produces reactive sites on the polymer backbone, and also small amounts of fluorine increase the concentration of atomic oxygen in the plasma.

Based on these considerations, an integrated circuit (IC) compatible process to fabricate nitride optical waveguides is presented. Results shown in this work demonstrate that a SF<sub>6</sub>/O<sub>2</sub> fluorine chemistry mixture in ECR plasma source and low substrate temperatures at about  $-30\text{ }^{\circ}\text{C}$  can successfully etch a 0.4  $\mu\text{m}$  deep nitride rib waveguide having width in the 2  $\mu\text{m}$  range. Furthermore, the combination of a hard 100 nm thick SiO<sub>2</sub> mask with a standard positive PR Shipley S1811 mask substantially improved etching parameters and increased allowable etching time. The process was optimized to obtain a good selectivity of nitride over the mask, with highly anisotropic etching, demonstrating nitride profiles with vertical sidewalls.

## II. EXPERIMENTAL SETUP

Silicon starting substrates with 3.5  $\mu\text{m}$  thermal oxide were used. A low stress, low refractive index ( $n=1.95$ ), plasma enhanced chemical vapor deposition Si<sub>3</sub>N<sub>4</sub> film of

<sup>a)</sup>Author to whom correspondence should be addressed; electronic mail: dcelo@doe.carleton.ca

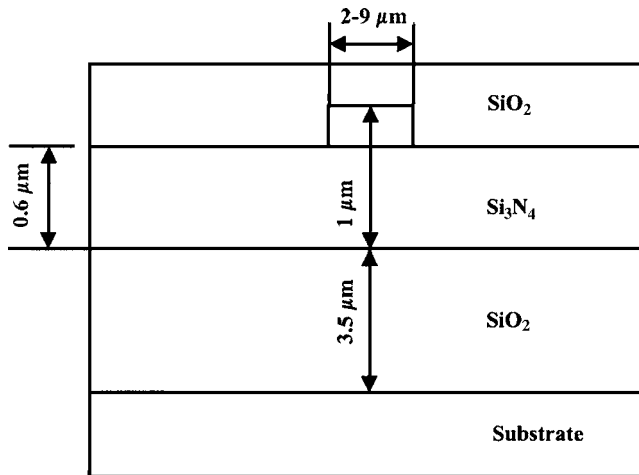


FIG. 1. Waveguide structure.

1 μm thickness was deposited. The thermal oxide layer serves as a buffer or underclad for the nitride WG core, as schematically shown in Fig. 1.

### A. Lithography and plasma etching

Two different etch masks were considered: (a) a standard single layer positive PR S1811; and (b) a two layer mask with the first layer being a 100 nm thick oxide, covered by a second layer of PR S1811. The only difference between these two experiments is the addition of the oxide hard mask, which should increase the process selectivity of Si<sub>3</sub>N<sub>4</sub> over SiO<sub>2</sub> by acting as an etching barrier.<sup>11</sup> Waveguides of different rib widths (2–5 μm) were patterned using a standard lithography process.

At this point, wafers with and without an oxide-mask layer were separated. An additional lithography step was required for wafers having the 100 nm SiO<sub>2</sub> mask layer. The pattern was transferred into the oxide layer by anisotropic dry etching, which was completed for 3 min in a reactive ion etcher (RIE) with CHF<sub>3</sub>/O<sub>2</sub> gas flows of 42.5/7.5 SCCM (SCCM denotes cubic centimeter per minute at STP), respectively. Etched structures were investigated by optical microscopy, whereas the etch depth was measured with a Tenkor P1 profiler. Si<sub>3</sub>N<sub>4</sub> channels exposed for further plasma etching showed etch depth of 180 nm (100 nm of SiO<sub>2</sub> and 80 nm of Si<sub>3</sub>N<sub>4</sub>), leaving the rest of the wafer area covered by a two layer (oxide/PR) mask.

Plasma etching was completed using a PlasmaTherm 720 ECR etcher with a SF<sub>6</sub>/O<sub>2</sub> chemistry and substrate cooling maintained by a temperature controller. Cooling was provided by a continuous flow of helium gas across the back side of the wafer. The helium was precooled through a heat exchanger filled with liquid nitrogen. The wafer was clamped against an O-ring seal to prevent the escape of the helium into the vacuum chamber.

The PlasmaTherm system was designed for use with 100 mm diameter wafers. However, waveguides presented in this work were fabricated in small pieces (typically 1 × 1 cm<sup>2</sup>). During the etching process in ECR, these small

pieces were attached to a backing wafer using SPI Supplies double sided adhesive conductive carbon tape. The backing wafer and the attached sample were clamped to the cooled chuck, facilitating the cooling action. Gas flow rates into the chamber are mass-flow controlled. The flow ratio SF<sub>6</sub>/O<sub>2</sub> = 3.65/2.21 SCCM was previously adjusted to maximize the etch rate and kept constant during the etching process. The operating pressure was 6 mTorr.

In addition to low temperature etching, several etching experiments were completed at room temperature. Samples were attached to the backing wafer with and without carbon tape, leading to two different etching temperatures. The purpose of this experiment was to investigate the effect of temperature on etch rate, anisotropy, and selectivity. After etching, the PR layer was ashed in oxygen plasma using a PlasmaPreen system, while the SiO<sub>2</sub> mask was left in place. Samples were examined in a JEOL JSM-6400 SEM operated at 20–25 kV.

### B. Wafer and sample temperature measurements

The actual temperature of the sample is an important parameter, especially since low temperature plasma etching is involved in the experiments. In addition, the use of carbon tape to attach a sample on a cooled wafer introduces a temperature difference that might affect how the results can be applied to other situations. Therefore, an experiment to measure temperature on the surface of a dummy wafer and two samples (attached to the wafers with and without carbon tape) was set up. This would make possible a comparison between wafer surface temperature and the temperature of the sample piece with and without carbon tape. Photographs of the experimental setup are shown in Fig. 2, where Fig. 2(a) depicts the backing wafer and two samples attached to the wafer with and without carbon tape. The sample in the upper part of the picture has no carbon tape underneath, thus, polyimide tape (Kapton) was used to hold it in place. Three self adhesive type K thermocouple (TC) probes from OMEGA Corp. with temperature range of –200–1250 °C and standard limits of error 0.75% were attached to both samples and wafer surfaces as shown. A six-pin port on the ECR etcher [Fig. 2(b)] was dedicated for thermocouple wires to the handheld unit (OMEGA HHM25-TC) connection, allowing temperature readings at all three channels.

## III. RESULTS AND DISCUSSION

Dry etching plasma process of Si<sub>3</sub>N<sub>4</sub> optical rib waveguide dictates three main requirements: anisotropic etching with high aspect ratio to minimize the lateral underetch, good selectivity to mask material, and high etch rate of nitride. In the following, all these requirements are investigated. The optimum parameters of the etching process were identified with preliminary experiments and are shown in Table I; unless otherwise mentioned, these parameters were kept constant in all of the following experiments.

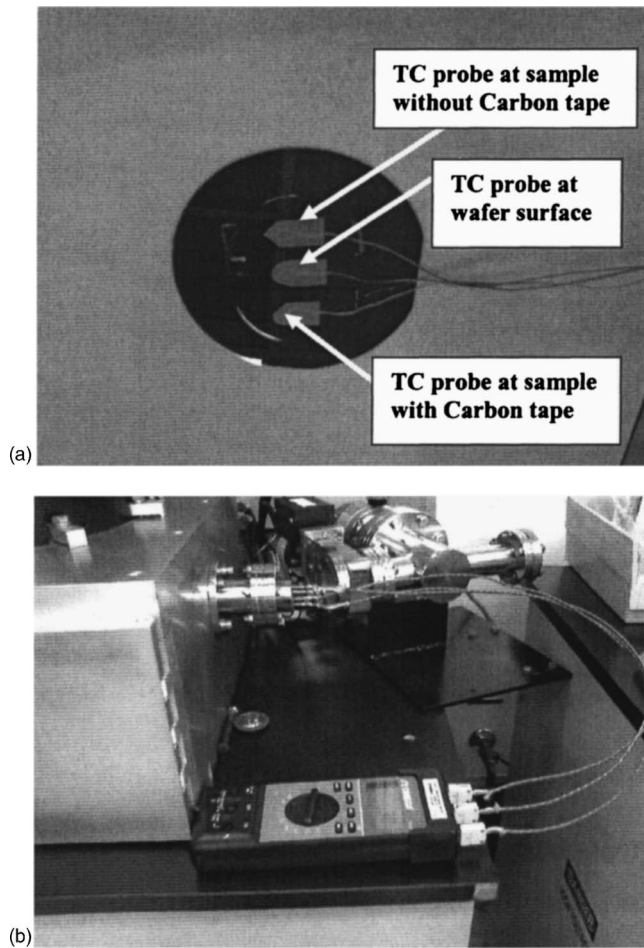


FIG. 2. Experimental setup for wafer and sample surface temperature measurement: (a) a thermocouple probe has been attached to the surface of each sample (upper and lower) and wafer (in the middle), with wires running to the six-pin port, and (b) a three-channel handheld unit connected to the port making possible temperature readings from all three probes.

### A. Temperature measurement

The experiment was performed at chuck temperatures of  $-31$  and  $-81$  °C, with all other etching parameters as shown in Table I. Plasma was turned “on” for 2 min; longer etching time was not advisable due to temperature limitations in TC probe adhesives and connecting wires. Temperature reading was performed immediately after the etching plasma was

TABLE I. Etch parameters for etching experiments at two different temperatures.

Chuck temperature (°C)	-30	21
Microwave power (W)	305	303
Microwave reflected power (W)	3	3
rf forward power (W)	10	10
Base pressure (Torr)	$1.5E-6$	$15E-6$
Operating pressure (mTorr)	6	6
SF <sub>6</sub> /O <sub>2</sub> gas flow (SCCM)	3.65/2.21	3.65/2.21

turn off. Readings from chuck temperature controller, wafer surface, and both sample surfaces are summarized in Table II.

As evident from the results, the temperature offset between these two attachment methods is large. Carbon tape adhesive with its high thermal conductivity provides an excellent path for heat dissipation toward the cooled wafer. There is no temperature difference between the carrier wafer and the sample attached with carbon tape, allowing the etching process to be at a truly low temperature. In contrast, there is a large offset between the temperature of the sample attached with Kapton tape and that of the carrier wafer. The thin evacuated layer between this sample and the carrier wafer acts as a thermal barrier, blocking heat flow. Also of interest is the temperature offset between the controller temperature readings and the wafer surface, which is due to the controller probe location being different from the location of the TC probe attached to the wafer surface. This offset is relatively small compared to the offset between the wafer surface and the sample without carbon tape and, as a result, it can be neglected. However, it becomes important and should be taken into account when samples attached with carbon are etched.

### B. Low temperature plasma etching

A sample with one layer of PR mask was patterned and attached to the backing wafer with carbon tape. The etching process was completed for 10 min at chuck temperature of  $-30$  °C. The addition of O<sub>2</sub> into the SF<sub>6</sub> gas flow makes anisotropic etching possible at wafer temperatures much higher than the  $-130$  °C reported in Ref. 5. The aspect ratio

TABLE II. Temperature readings from chuck temperature controller, wafer surface, and sample surface for samples attached to the wafer with and without carbon tape.

Measurement	Measurement Time	Temperature (°C)			
		Chuck	Wafer surface	Sample without carbon tape	Sample with carbon tape
1	Before etching	-31	-40.3	-30.4	-39.8
	After etching	-30	-38	+130	-37
2	Before etching	-81	-78	-69	-78
	After etching	-77	-80	+138	-77

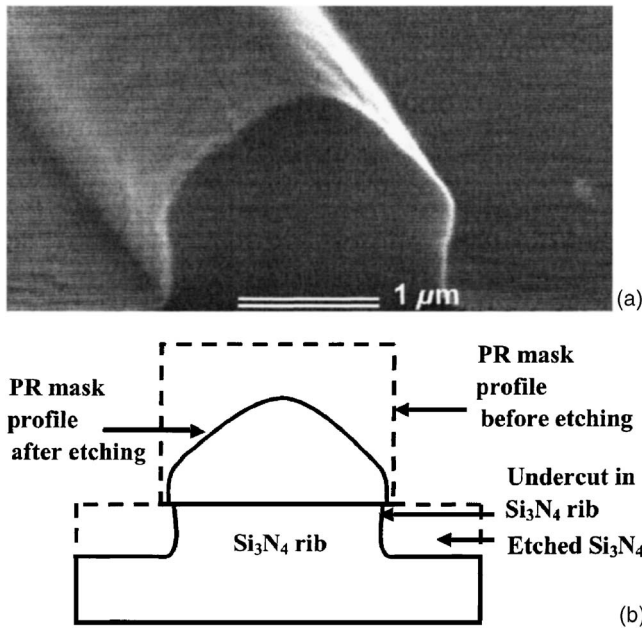


FIG. 3.  $\text{Si}_3\text{N}_4$  rib waveguide profile after 10 min etch in ECR with  $\text{SF}_6/\text{O}_2$  gas chemistry and wafer temperature at  $-30^\circ\text{C}$ ; (a) SEM image, and (b) a schematic representation of the PR mask profile before and after etching, resist/nitride interface and undercut, and PR erosion (both top and sidewall).

obtained in the process is 5:1, resulting in satisfactory anisotropy. A scanning electron microscopy (SEM) image of a cleaved sample depicting a rib profile of  $\text{Si}_3\text{N}_4$  waveguide with PR mask is shown in Fig. 3(a). For clarity, a schematic representation of the PR mask profile before and after etching as well as resist-nitride interface and undercut in the nitride rib is shown in Fig. 3(b). Of course, the  $\text{SF}_6/\text{O}_2$  etching relies on sidewall passivation with oxide or oxyfluoride, forming a barrier in the sidewalls and limiting further etching. As a result, reasonably anisotropic etching with relatively vertical and smooth sidewalls was demonstrated. However, mask erosion and lateral undercutting around 80 nm are noticeable. This could be due to carbon compounds in the photoresist released in the process; these organics react to remove the sidewall passivation, giving lateral undercutting as shown in the rib profile.

Unfortunately, the addition of oxygen into the gas flow reduces the selectivity of nitride to resist, limiting etching time and potential depth of the trench. The mechanism is based on incorporation of atomic oxygen into polymer which weakens bonds between adjacent carbons. Oxygen also significantly increases the fluorine-free radical production in the plasma, hence increasing the resist etch rate as well as making the etch profile more isotropic. The remaining overall thickness and the highly slanted sidewalls of the PR layer (Fig. 3) demonstrate poor selectivity in the process. Measurement of the etch depth reveals 0.8:1 selectivity of  $\text{Si}_3\text{N}_4$  over PR, with corresponding etch rates of 36 and 44 nm/min.

In order to improve selectivity in the process an oxide hard mask of 100 nm thick was deposited over the silicon nitride layer. Previous experimental work carried out in our

ECR etcher with parameters consistent with this process has demonstrated selectivity of 4.6:1 of  $\text{Si}_3\text{N}_4$  over  $\text{SiO}_2$ . Therefore, a patterned oxide layer can serve as a hard mask for nitride WG etching. It should be noted here that at the end of the process, this oxide mask does not need to be removed; instead, it can serve as part of the oxide overcladding, a necessary step in further processing of buried waveguides. Etching of  $\text{Si}_3\text{N}_4$  was performed for 8 min with plasma parameters shown in Table I. After removing the resist, with the  $\text{SiO}_2$  mask left in place, the overall etch depth was found to be 480 nm with etch uniformity  $\pm 1.4\%$  measured across a 10 mm sample, achieving 300 nm  $\text{Si}_3\text{N}_4$  etched in this process (recall that 180 nm was previously etched in RIE), with etch rate of 37.5 nm/min.

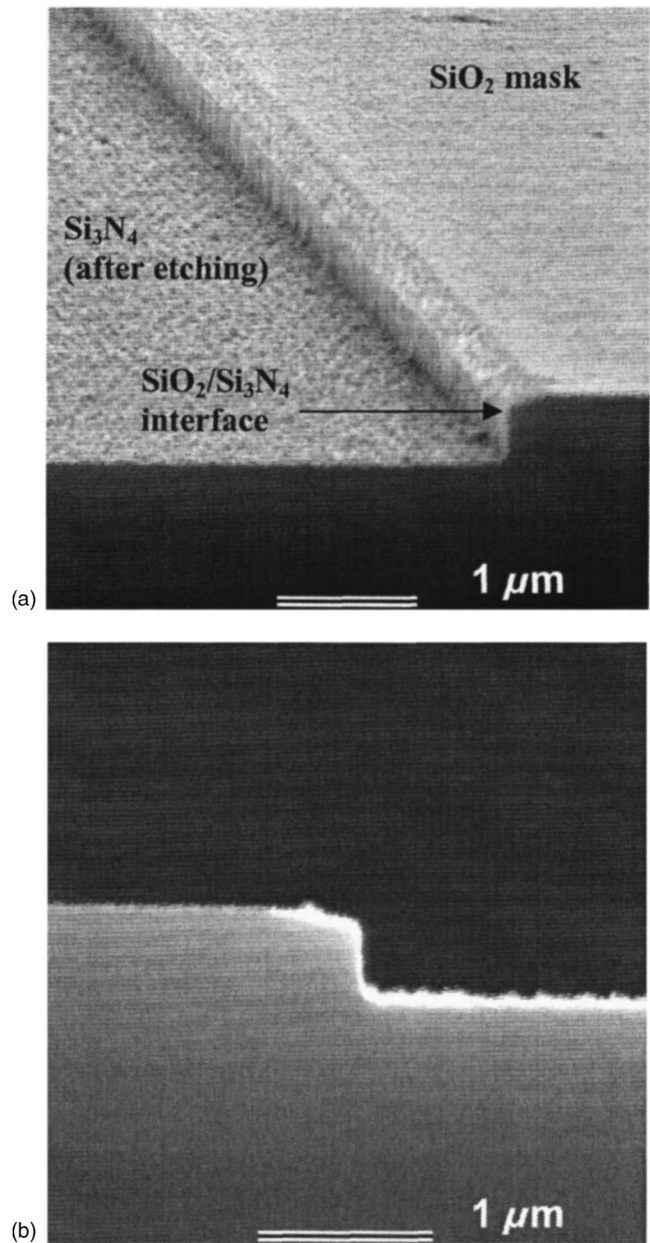


FIG. 4. SEM image of oxide-masked waveguide; (a) vertical sidewall demonstrating highly anisotropic etching, and (b) rib profile including 100 nm silicon dioxide layer and 300 nm silicon nitride.

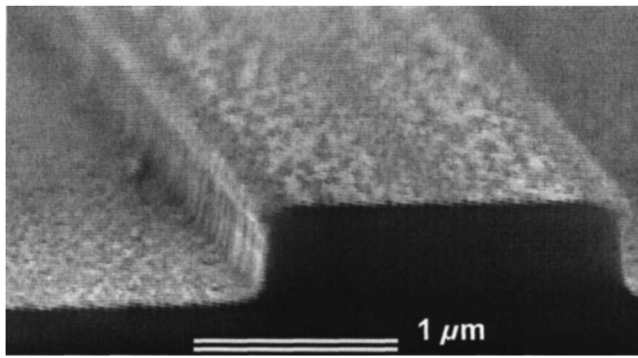


FIG. 5. SEM image of cleaved waveguide from sample A. Rib profile shows around 100 nm undercutting.

Figure 4 shows a SEM image of a cleaved waveguide. Verticality of the sidewall demonstrates highly anisotropic etching, with no signs of oxide-mask erosion or undercutting. Also, as expected, selectivity for silicon nitride over oxide is very good, with the oxide hard mask being very effective. However, due to our oxide etching process not being very anisotropic, slanted edges at the oxide cap of the rib profile can be seen. Fortunately, these slanted edges are limited to  $\text{SiO}_2$  layer of thickness of 100 nm and do not affect the  $\text{Si}_3\text{N}_4$  layer and the waveguide core itself.

### C. Temperature dependent etching process

Further investigation of temperature dependent silicon nitride etching was completed through another etching experiment. Similar to the previous experiment, two patterned samples with oxide/PR mask were attached to the backing wafer: one with carbon tape adhesive (sample A) and one without any special adhesion or contact aid (sample B). While the chuck temperature controller was set at 21 °C, the other parameters remain the same, as shown in Table I. Under these conditions, etching was done for 8 min with the following results.

A cleaved waveguide image from sample A is shown in Fig. 5, where poor anisotropic etching and 100 nm silicon nitride undercutting demonstrate a strong temperature sensitivity of the process. This predictable trend can be explained by desorption of the deposited inhibitor layers which increases with temperature, resulting in a negative dependence of inhibitor deposition with temperature.<sup>12</sup> The overall etch depth of 520 nm was measured, with  $\text{Si}_3\text{N}_4$  etch rate of 42.5 nm/min. There is a 13.3% increase in the etch rate compared to the low temperature process.

Further, SEM images of WG ribs from sample B are shown in Fig. 6. A comparison between samples A and B shows no qualitative difference in etching results. However, some quantitative differences can be noticed. Besides more undercutting, a profile measurement confirms greater etch depth (580 nm) and etch rate of silicon nitride (50 nm/min) for sample B. This can be explained by the higher sample temperature during etching. As previously demonstrated, the carbon tape adhesive applied on sample A achieves good thermal contact between sample and backing wafer, lowering

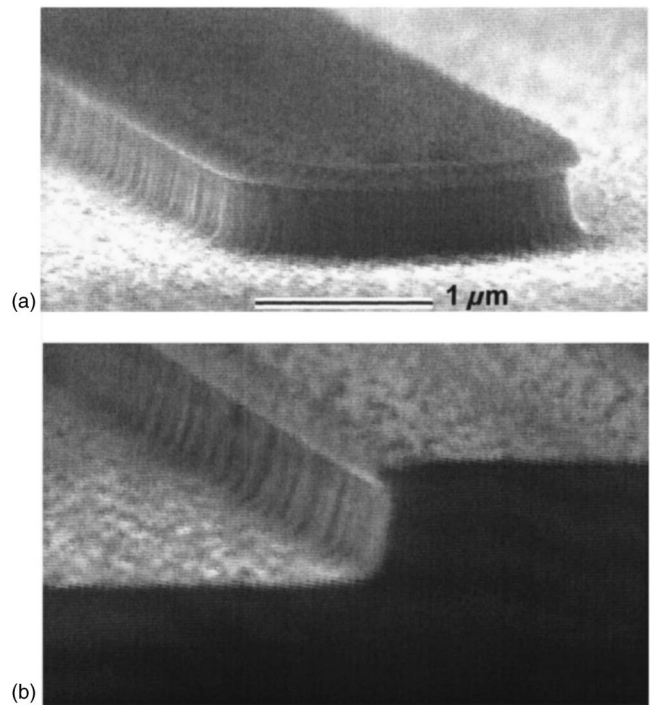


FIG. 6. SEM images of rib waveguides: (a) waveguide butt and (b) cleaved edge.

sample temperatures. In contrast, sample B is characterized by a poor thermal contact, allowing elevated temperatures in the sample.

In general, these results once more demonstrate a strong temperature effect on the etching process. Low wafer temperature plays an important role on anisotropic etching. As a practical application, low temperature etching has demonstrated improved characteristics for  $\text{Si}_3\text{N}_4$  waveguide etching.

### IV. CONCLUSIONS

It has been demonstrated that  $\text{Si}_3\text{N}_4$  waveguides can be fabricated successfully by combining ECR plasma etching at wafer temperature of  $-30$  °C and  $\text{SF}_6/\text{O}_2$  gas chemistry with the application of a  $\text{SiO}_2$  hard mask of thickness of 100 nm. Etching is highly anisotropic with vertical sidewalls and no undercutting. The etch rate of 37.7 nm/m achieved in these experiments is acceptable for etching silicon nitride waveguides. The effect of temperature on etch rate and other parameters was also investigated. Results show that sample surface temperature strongly affects both the etch rate and the anisotropy in the process. By lowering this temperature, the anisotropy can be improved.

### ACKNOWLEDGMENTS

This work was supported by the Natural Sciences and Engineering Research Council of Canada (NSERC) and by the Canada Research Chairs program.

<sup>1</sup>C. R. Betanzo, S. A. Moshkalyov, and J. W. Swart, *J. Vac. Sci. Technol. A* **21**, 461 (2003).

- <sup>2</sup>K. M. Chang, T. H. Yeh, I. C. Deng, and H. C. Lin, *J. Appl. Phys.* **80**, 3048 (1996).
- <sup>3</sup>R. Legtenberg, H. Jansen, M. de Boer, and M. Elwenspoek, *J. Electrochem. Soc.* **142**, 2020 (1995).
- <sup>4</sup>G. Craciun, M. A. Blauw, E. Van der Drift, P. M. Sarro, and P. J. French, *J. Micromech. Microeng.* **12**, 390 (2002).
- <sup>5</sup>S. Tachi, K. Tsujimoto, and S. Okudaira, *Appl. Phys. Lett.* **52**, 616 (1988).
- <sup>6</sup>A. G. Rickman, G. T. Reed, and F. Namavar, *J. Lightwave Technol.* **12**, 1771 (1994).
- <sup>7</sup>M. Boufnichel, S. Aachboun, F. Grangeon, P. Lefauchaux, and P. Ranson, *J. Vac. Sci. Technol. B* **20**, 1508 (2002).
- <sup>8</sup>M. A. Blauw, T. Zijlstra, R. A. Bakker, and E. van der Drift, *J. Vac. Sci. Technol. B* **18**, 3453 (2000).
- <sup>9</sup>I. Hasan, C. A. Pawlowicz, L. P. Berndt, and N. G. Tarr, *J. Vac. Sci. Technol. A* **20**, 983 (2002).
- <sup>10</sup>D. M. Manos and D. L. Flamm, *Plasma Etching: An Introduction* (Academic, London, 1989).
- <sup>11</sup>M. Matsui, F. Uchida, M. Kojima, T. Tokunaga, F. Yano, and M. Hasegawa, *J. Vac. Sci. Technol. A* **20**, 117 (2002).
- <sup>12</sup>J. D. Plummer, M. D. Deal, and P. B. Griffin, *Silicon VLSI Technology—Fundamentals, Practice and Modeling* (Prentice Hall, Upper Saddle River, NJ, 2000), pp. 640–646.